Journal scientific and applied research, vol. 5, 2014
Association Scientific and Applied Research
International Journal

*Original Contribution*

ISSN 1314-6289

# $Al^{3+}$ ACCEPTORS AND THE OPTICAL PROPERTIES OF $Bi_{12}SiO_{20}$:Cr+Al

**P. Petkova, P. Vasilev**

*SHUMEN UNIVERSITY "KONSTANTIN PRESLAVSKY", 115 UNIVERSITETSKA STREET, 9712 SHUMEN, E-MAIL: PETYA232@ABV.BG*

***Abstract:*** *Absorption measurement is taken in the visible spectral region (650 – 850 nm). The dopants $Cr^{3+}$ and $Al^{3+}$ ions occupy the tetrahedral sites in the crystal lattice of doped sillenite. The electron transitions in $Cr^{3+}$ are presented in the case of $Bi_{12}SiO_{20}$:Cr and $Bi_{12}SiO_{20}$:Cr+Al. The total cross-section $\sigma_a$ of combined chromium-aluminium absorption structure and the spin-orbit coupling energy of $Cr^{3+}$ are calculated.*

***Key words:*** *absorption spectrum, 3d transition metals, total cross-section of impurity absorption, spin-orbit coupling energy*

## INTRODUCTION

Bismuth oxide compounds such as the sillenite-type $Bi_{12}MO_{20}$ (BMO, where M = Si, Ge, Ti) crystals are being extensively studied because of their potential applications including dynamic holography, optical information processing, optical phase conjugation and real-time interferometry [1–5]. The defect identification, including the dopant ions involved, their valence and local symmetry is essential because this information may guide the efforts for optimization of the synthesis conditions to obtain the intended material properties. In this paper, we present a detailed optical study of $Cr^{3+}$ and $Cr^{4+}$ ions which are in the tetrahedral coordination.

## MATERIALS AND SAMPLES PREPARATION

$Bi_{12}SiO_{20}$ crystals belong to the sillenite family of materials with the space symmetry I23 with a body centered cubic unit cell (a = 10.102 Å), which contains 24 $Bi^{3+}$ ions, 2 $Si^{4+}$ ions and 40 $O^{2-}$ ions (nominal valences). Two structural elements can be distinguished, the $SiO_4$ regular tetrahedron and the $BiO_7$ polyhedron [6]. The former exists at the corners and at the center of the cubic unit cell. In the $BiO_7$ polyhedron, each of the $Bi^{3+}$ ions is surrounded by 7 oxygen atoms and is coordinated in a pseudo-octahedral configuration, in which the oxygen atom at one corner is replaced by two atoms at somewhat larger

distance. BSO single crystals were grown in air by the Czochralski method from a melt containing a mixture of high purity (99.9999%) oxides including $Bi_2O_3$ and $SiO_2$ in a 6:1 molar ratio [7]. Platinum crucibles of 60 mm in diameter and 80 mm in height were used as containers. The crystals were grown in a <001> direction under conditions of low temperature gradient over the solution (5–7 $^oC$/cm), at a growth rate of 0.7 mm/h and a rotation rate of 20 rpm. Fully facetted and optically homogeneous crystals of 35 mm in diameter and 50 mm in height were obtained. The starting chromium and aluminium dopants were introduced into the melt solution in the form of $Cr_2O_3$ and $Al_2O_3$ oxides. The analysis by atomic absorption spectrometry shows that they are present in the crystal at concentration of [Cr] = $7{,}2x10^{20}$ $cm^{-3}$ and [Al] = $2{,}2x10^{20}$ $cm^{-3}$.

## EXPERIMENTAL RESULTS AND DISCUSSION

The basic structural building units of solid oxides are $MO_6$ metal-oxygen octahedra and, possibly, additional $MO_4$ tetrahedra. The complete crystal structure is built up of corner-, face- and/or edge-sharing connections of these structural elements. Additional cations (A) can be incorporated at interstitial lattice sites. These are increasingly formed, the more open-structured the whole network of $MO_n$ units appears to be. Generally, open crystal structures imply high formal M-cation charge states (referring to formal $O^{2-}$ anions) leading to mixed ionic-covalent (or semiionic) material properties. The M-cations are in most cases transition-metal (TM) ions.

Charge carriers, either valence-band (VB) holes or conduction-band (CB) electrons, are created by doping with impurities, annealing treatments or by light-induced charge-transfer excitations which, for example, take place during photorefractive processes in the appropriate oxides.

The present work initiates a systematic and detailed characterization of localized hole states in complex oxides.

Our investigations employ real-space embedded-cluster calculations, which consistently combine electron correlations and defect-induced lattice relaxations. This procedure is indispensable in order to predict the richness of possible hole

states. The trapping of holes at acceptor defects leads to a localization of hole states, which is further aided by defect induced lattice distortions.

Principally, there is “on-acceptor” and “off-acceptor” hole trapping. In the first case the trapped hole localizes at the acceptor site (thereby increasing the acceptor charge state by one positive unit, i.e. $M^{+n} + h \rightarrow M^{+(n+1)}$), and in the second case the hole remains at the oxygen ligands. Further, the off-acceptor case allows to classify hole states according to their degree of delocalization, i.e. complete localization at exactly one ligand anion, intermediate localization at two neighboring oxygen ions ($V_k$ centers), and delocalization over more than two oxygen ligands. Which hole-localization type is favored depends on the

ionicity of the host system, but also on the incorporation site and electronic structure of the acceptor. Such species could explain the diamagnetic hole centers in photorefractive oxides [8].

In comparison to most TM acceptors the hole localization properties can differ at ionic acceptor cations due to the lack of filled acceptor levels above the VB edge and of covalent charge transfer. The situation is even worse for completely delocalized states. Again electron correlation supports hole delocalization. Most favorable are the delocalized state and the formation of $V_k$ centers. However, there is no clear indication in favor of the latter species. But the results suggest a delicate balance between the local electronic structure and defect-induced lattice distortions: Increasing the acceptor ionicity would lead to localized off-acceptor holes, whereas a reduced ionicity implies hole delocalization. In an intermediate small "window" the formation of $V_k$ centers might be most favorable. This also explains why $V_k$ centers are rarely observed in oxides. Interestingly, $V_k$ centers have been also proposed in $Al_2O_3$ [9].

The electron paramagnetic resonance (EPR) identifies a chromium ion in the unusual $Cr^{3+}$ valence replacing a substitutional $Si^{4+}$ in tetrahedral oxygen coordination [10]. Evidence is found that the symmetry lowering from tetrahedral ($T_d$) to trigonal ($C_{3v}$) is not spontaneous, but induced by an associated defect. The aim of this work is to explain the influence of acceptor $Al^{3+}$ on the absorption structure of $Cr^{3+}$ in the spectral region 650-850 nm.

The experimental set up for measurement of the absorption coefficient in the visible and near IR region consists of the following: a halogen lamp with a stabilized 3H-7 rectifier, a SPM-2 monochromator, a system of quartz lenses, a polarizer, a crystal sample holder, and a Hamamatsu S2281-01 detector.

The absorption coefficient of investigated samples has been measured to be between 650 and 850 nm (Figs.1a and 2a). The first derivative of absorption coefficient at photon energy is calculated to be in the spectral region 640-850 nm. The $[d\alpha/d(h\nu)]$ determines only the number of electron transitions in a $Cr^{3+}$ ions and it does not give an exact information about the energy position of these transitions. This is the reason for the calculation of second derivative of absorption coefficient $[d^2\alpha/d(h\nu)^2]$.

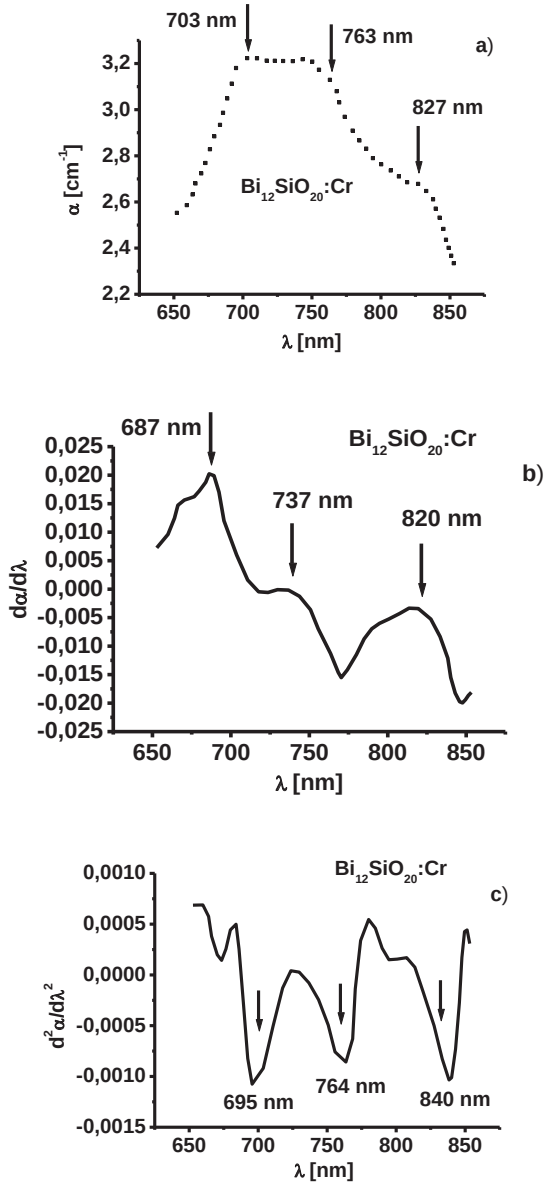


Figure 1 a) Absorption spectrum of $Bi_{12}SiO_{20}:Cr^{3+}$ in the spectral region 650 – 850 nm; b) the first derivative of absorption coefficient; c) the second derivative of absorption coefficient.

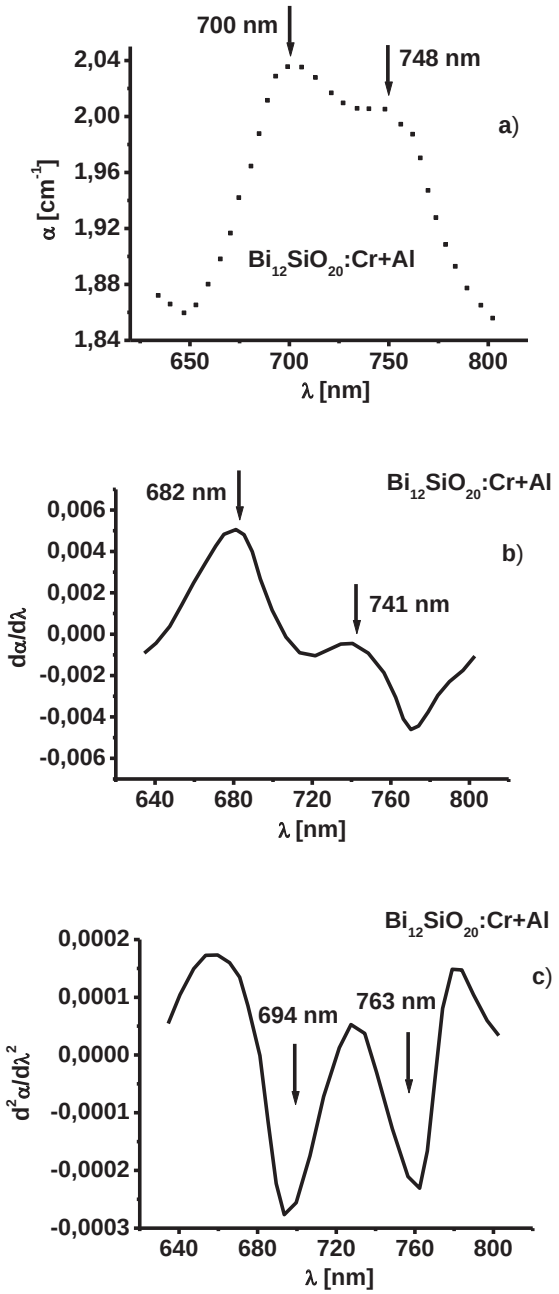


Figure 2 a) Absorption spectrum of $Bi_{12}SiO_{20}$:Cr+Al in the spectral region 640 – 800 nm; b) the first derivative of absorption coefficient; c) the second derivative of absorption coefficient

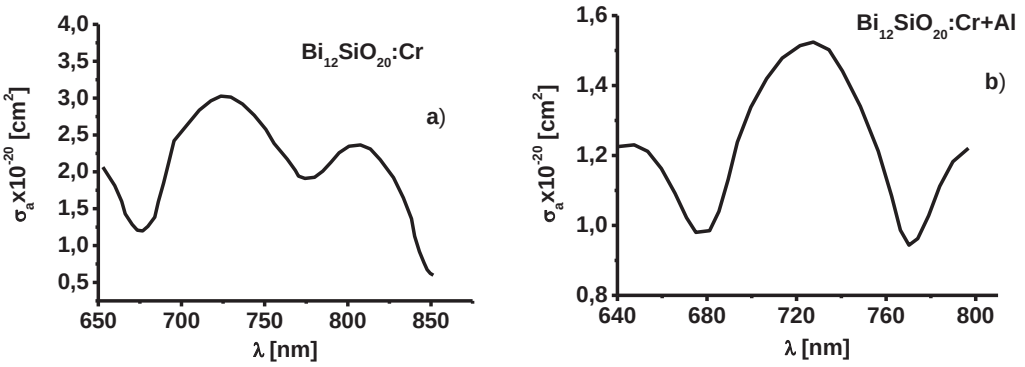


Figure 3 The total cross-section $\sigma_a$ of impurity absorption in the case of: a) $Bi_{12}SiO_{20}$:Cr; b) $Bi_{12}SiO_{20}$:Cr+Al.

The absorption coefficient is calculated using the formula: (1) $\alpha = (1/d)ln(I_0/I)$,

where $I_0$ is the intensity of incident light, I is the intensity of passing light and d is the sample thickness.

The components of $Cr^{3+}$ structure that are connected with the electron transitions are $^4A_2(^4T_1(^4F)) \rightarrow {}^2E(^2G)$, $^4A_2(^4T_1(^4F)) \rightarrow {}^4A_1(^4T_2(^4F))$ and $^4A_2(^4T_1(^4F)) \rightarrow {}^2E(^2T_1(^2G))$ [11]. The components of combined chromium-aluminium structure that are connected with the electron transitions are respectively $^4A_2(^4T_1(^4F)) \rightarrow {}^4A_1(^4T_2(^4F))$ and $^4A_2(^4T_1(^4F)) \rightarrow {}^2E(^2T_1(^2G))$. This fact is due to the presence of $Al^{3+}$ in the sillenite.

If the electron transitions are realized between the basic and the closest low energy excited states, then they are connected with the manifestation of the dynamical Jahn-Teller effect [11]. This effect is manifested as the deformation of chromium tetrahedron and the $T_d$ symmetry transforms into the $C_{3v}$ symmetry. The ionic radii of $Si^{4+}$, $Cr^{3+}$ and $Al^{3+}$ are as follow 0.40 Å, 0.755 Å and 0.675 Å. Thus it can be observed the tetrahedral distention. The final result is expressed by the great influence of Jahn-Teller effect on the energy values of observed impurity absorption bands [11] and the chromium complex becomes stable under the influence of spin-orbit interaction.

After the spin-orbit interaction the total angular momentum J becomes equal to 1/2 and 3/2. The EPR of chromium doped $Bi_{12}SiO_{20}$ gives information that the total spin angular momentum S is 3/2 [10]. In this connection, they are two possibilities for the total orbital angular momentum L = 0 and L = 1. The case when L = 1 is very interesting, because the orbital quantum number l = ±1. The spin-orbit coupling energy is given by the equation:

$$(2) \quad E_{so} = \frac{Z^4}{2(137)^2 n^3}\left(\frac{j(j+1) - l(l+1) - s(s+1)}{2l(l+1/2)(l+1)}\right)$$

In this connection, the values of spin-orbit coupling energy for $Cr^{3+}$ are as follow (table 1):

Table 1

| quantum numbers of $Cr^{3+}$ | $E_{SO}$ [eV] |
|---|---|
| n=2, l=1, j=1/2, s=3/2 | -0,9206 |
| n=2, l=1, j=-1/2, s=-3/2 | -0,5524 |
| n=2, l=1, j=±3/2, s=±3/2 | -0,3682 |

The cross-section of the impurity absorption is of great significance for the application of doped materials in practice [12]. It is used to estimate how radiation is absorbed by the impurity ions in the crystals. The total cross-section $\sigma_a$ of the impurity absorption is determined by the integration of the impurity ions within the absorption band

$$(3) \qquad \sigma_a = \frac{1}{N}\int_{E_1}^{E_2} \alpha(E)\, dE$$

Where:

N is the number of the impurity ions in the unit volume;

α is the impurity absorption coefficient, typical for the energy interval from $E_1$ to $E_2$. The total cross-section $\sigma_a$ of chromium and aluminium absorption as a function of wavelength is presented in fig. 3.

## CONCLUSIONS

1) $Al^{3+}$ ions are $V_k$ centers in the crystal lattice of double doped BSO.

2) The electron transition at 827 nm in $Cr^{3+}$ does not manifest in the combined chromium-aluminium absorption structure.

3) The total cross-section of combined chromium-aluminium absorption has smaller values and it has narrow spectral region in comparison with $\sigma_a$ of chromium ions.

## ACKNOWLEDGMENTS

Partial financial support by project of Shumen University (2014) is gratefully acknowledged.

REFERENCES


[1] Y. H. Ja, Opt. Commun. 42, 377 (1982).
[2] M. P. Georges, V. S. Scauflaire, and P. C. Lemaire, Appl. Phys. B 72, 761 (2001).
[3] E. A. Barbosa, R. Verzini, and J. F. Carvalho, Opt. Commun. 263, 189 (2006).
[4] M. R. R. Gesualdi, D. Soga, and M. Muramatsu, Opt. Laser Technol. 39, 98 (2007).
[5] E. A. Barbosa, A. O. Preto, D. M. Silva, J. F. Carvalho, and N. I. Morimoto, Opt. Commun. 281, 408 (2008).
[6] S. C. Abrahams, J. L. Bernstein, and C. Svensson, J. Chem. Phys. 71, 788 (1979); S. C. Abrahams, P. B. Jamieson, and J. L. Bernstein, ibid. 47, 4034 (1967).
[7] P. Sveshtarov and M. Gospodinov, J. Cryst. Growth 113, 186 (1991).
[8] E. Possenriede, P. Jacobs, H. Kr¨ose, and O. F. Schirmer. *Appl. Phys.* A55, 73 (1992).
[9] L. Kantorovich, A. Stashans, E. Kotomin, and P. W. M. Jacobs. *Int. J. Quant. Chem.* 52, 1177 (1994).
[10] I. Ahmad, V. Marinova, H. Vrielinck, F. Callens, and E. Goovaerts, Journal of Applied Physics 109, 083506-1 083506-7 (2011).
[11] P. Petkova, Journal Scientific and Applied Research, Vol. 2, 58 (2012).
[12] Optical Properties of Condensed Matter and Applications, Edited by Jai Singh, John Wiley & Sons (2006).